Bioelectrochemistry 146 (2022) 108109

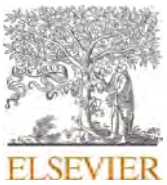

Contents lists available at ScienceDirect

Bioelectrochemistry

journal homepage: www.journals.elsevier.com/bioelectrochemistry

# Electrochemically switchable and tunable luciferase bioluminescence

Ali Othman, Evgeny Katz, Oleh Smutok

*Department of Chemistry and Biomolecular Science, Clarkson University, Potsdam, NY 13699-5810, USA*

ARTICLE INFO

*Keywords:*
Luciferase
Bioluminescence
Electrochemically switchable
Electrochemically tunable
Modified electrode

ABSTRACT

The biocatalytic activity of electrode-immobilized luciferase followed by bioluminescence emitted from the electrode surface was reversibly tuned and switched by applying electrochemical signals. When a reductive potential (−0.9 V vs. Ag/AgCl) was applied, $O_2$ was consumed at the electrode resulting in its depletion in a thin film near the electrode surface. This resulted in the inhibition of the immobilized luciferase which needs $O_2$ for the biocatalytic reaction. Releasing the potential resulted in diffusional equilibration of the $O_2$ local concentration with the bulk solution, then reactivating luciferase. Reversible inhibition-activation of luciferase was obtained upon cyclic application and releasing of the potential, respectively.

## 1. Introduction

Adaptivity of biological systems to variations in the environment is the key feature of life [1,2]. It is based on a multi-level and multi-mechanism regulation processes changing biochemical pathways and reaction kinetics in response to external signals. Artificial systems mimicking natural processes have very limited complexity and cannot reproduce even a small fraction of the natural features. While the present level of the artificial systems complexity is far from pretending to create an "artificial life", this complexity is already enough for numerous technological applications. Various "smart" systems, particularly for signal-triggered biomolecule release (e.g., drug release) [3], signal-controlled biofuel cell power production [4], signal processing in unconventional computing [5,6], signal-regulated porosity, optical features, diffusivity, etc., have been extensively studied in the last decades and reported in numerous papers and books. The signals applied to change the system properties include (bio)molecule inputs [7], light illumination [8], magnetic field [9] and electrical potentials [10] applied, etc. While the signal-responding systems may be designed in solutions [11] or immobilized states [12], particularly high attention has been given to the systems arranged at electrode surfaces [13], thus allowing functional integration between biomolecule assemblies and electronics. These studies have been recently performed in the framework of bioelectronics [14], particularly in the rapidly developed areas of implantable [15] and wearable [16] bioelectronics.

Immobilization of biomolecules (enzymes [17], antigens/antibodies [18], DNA/RNA [19]) at various surfaces (particularly at electrodes) has resulted in many practically important applications, especially in various biosensors [20,21]. The present study reports on a novel signal-controlled, switchable or tunable bioluminescence system based on luciferase enzyme immobilized at an electrode surface. The signals controlling the luciferase activity, measured as the light emission, were applied electrochemically, thus allowing the electronic control over the bioluminescence. While the present system does not aim at any immediate application, the concept demonstrated in the study may find practical applications, particularly taking into account that luciferase is an active component of various biosensors [22–24] and is used as a tool in molecular and cell biology [25] and in biotechnology [26].

## 2. Experimental section

### 2.1. Chemicals, materials and consumables

Luciferase (Lucif, E.C. 1.14.14.3, from *Vibrio fischeri*, Photobacterium f), adenosine triphosphate (ATP), hydrogen tetrachloroaurate (III) hydrate ($HAuCl_4$), and cysteamine were purchased from MilliporeSigma (formerly, Sigma–Aldrich). D-Luciferin was purchased from Selleckchem.com (chemical retailer). 4-(2-Hydroxyethyl)-1-piperazineethanesulfonic acid (HEPES buffer), 2-amino-2-(hydroxymethyl) propane-1,3-diol (TRIS buffer), sodium sulfate ($Na_2SO_4$), and glutaric dialdehyde (25 % v/v) were purchased from Acros Organics (Carlsbad, CA). All other standard organic and inorganic reagents were purchased from MilliporeSigma. All chemicals were purchased with the highest grade and were used without further purification. A pH sensitive fluorescent dye 3,4′-dihydroxy-3′,5′-*bis*-(dimethylaminomethyl)flavone (FAM345) [27] was synthesized as reported previously by our group

*E-mail addresses:* aothman@clarkson.edu (A. Othman), ekatz@clarkson.edu (E. Katz), osmutok@clarkson.edu (O. Smutok).

https://doi.org/10.1016/j.bioelechem.2022.108109
Received 28 December 2021; Received in revised form 10 March 2022; Accepted 22 March 2022
Available online 25 March 2022

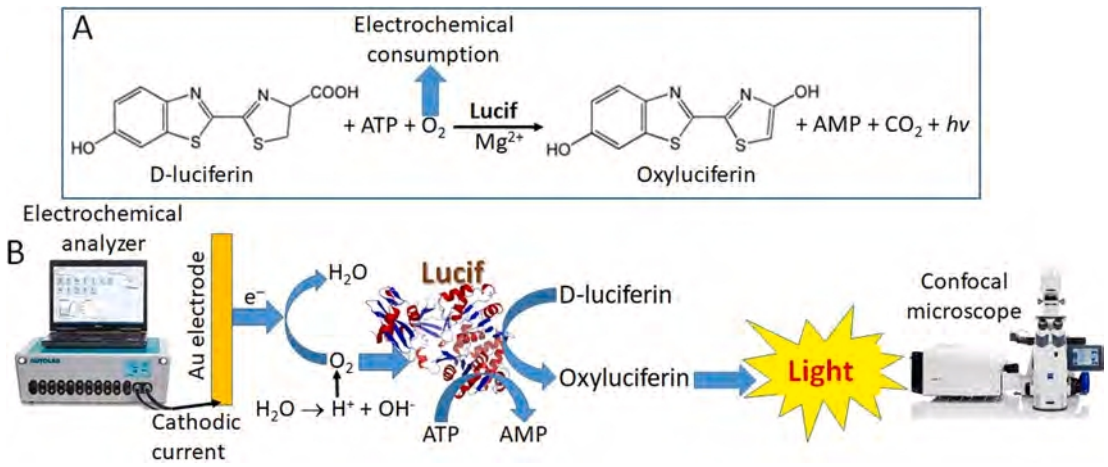


**Scheme 1.** (A) Luciferin oxidative transformation catalyzed by luciferase (Lucif) enzyme resulting in the light emission (bioluminescence). (B) The bioluminescence catalyzed by the electrode-immobilized Lucif detected with a confocal microscope. Note that electrochemical reductive consumption of $O_2$ results in its depletion near the electrode surface, then inhibiting the enzyme-catalyzed reaction. The electrochemical $O_2$ reduction resulting in $H_2O$ production consumes $H^+$ ions, then possibly increasing local pH, if the buffer concentration is not high enough. Abbreviation: AMP is adenosine monophosphate; other abbreviations are explained in the text.

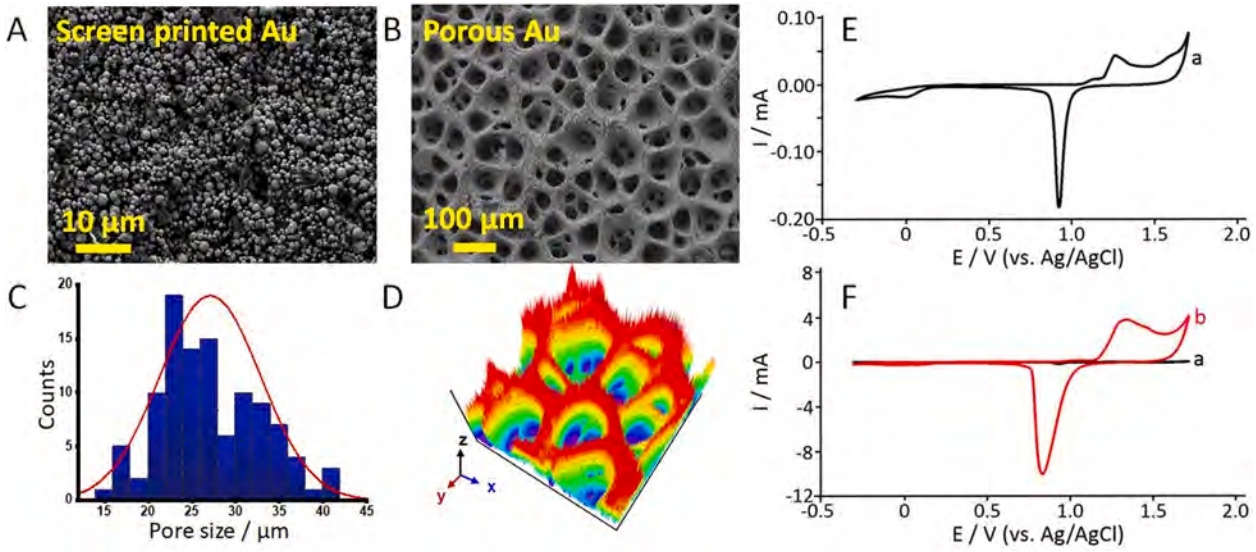


**Fig. 1.** Characterization of the highly porous gold (hPG) electrode used for immobilization of the luciferase enzyme. Scanning electron microscope (SEM) images of the original (as supplied) screen-printed gold electrode (SPGE) (A) and the highly porous gold (hPG) electrode (B). (C) The pore size distribution derived from the SEM image of the hPG electrode shown in (B). (D) 3D-surface mapping of the hPG electrode; the same electrode as shown in the SEM image in (B). Cyclic voltammograms obtained with the original SPGE (curve a in E and F) and with hPG electrode (curve b in F) in 0.5 M $H_2SO_4$, potential scan rate 100 mV/s. Note the different current scales in (E) and (F). The charge (integrated current) under the cathodic peaks in the cyclic voltammograms (E) and (F) is proportional to the real surface of the used Au electrodes.

[28]. All experiments were carried out using ultrapure water (18.2 MΩ•cm; Barnstead NANOpure Diamond).

### 2.2. Instrumentation

Electrochemical experiments were conducted using an electrochemical workstation (ECO Chemie Autolab PASTAT 10) and GPES 4.9 (General Purpose Electrochemical System) software. While performing electrochemical experiments (cyclic voltammetry) in an electrochemical cell, the potentials were measured using a BASi Ag|AgCl|KCl, 3 M, reference electrode, and a graphite slab was used as a counter electrode. The opto-electrochemical experiments (confocal microscope measurements) were performed using the internal Ag quasi-reference and counter electrodes associated with a screen-printed gold electrode (SPGE) assembly. Fluorescent images were obtained with a confocal microscope (Leica Confocal Microscope LM6, Leica Microsystems, Buffalo Grove, IL, USA). ImageJ software was used for quantifying color intensity of images, color distributions, and pore size analysis. pH values of the solutions were adjusted using a Mettler Toledo S20 SevenEasy pH meter. The surface morphology of the gold unmodified (as supplied) and modified SPGEs were visualized by field emission scanning electron microscopy (FE-SEM) using a JEOL JSM-7400F instrument.

### 2.3. Preparation of the porous gold electrodes

The screen-printed gold electrodes (SPGEs) were purchased from DropSens Metrohm (DRP 220BT, see the electrode composition at the company website: http://www.dropsens.com/en/screen_printed_electrodes_pag.html). The SPGE is composed of a Au working electrode (4 mm diameter, geometrical area ca. 0.13 $cm^2$) and include counter and

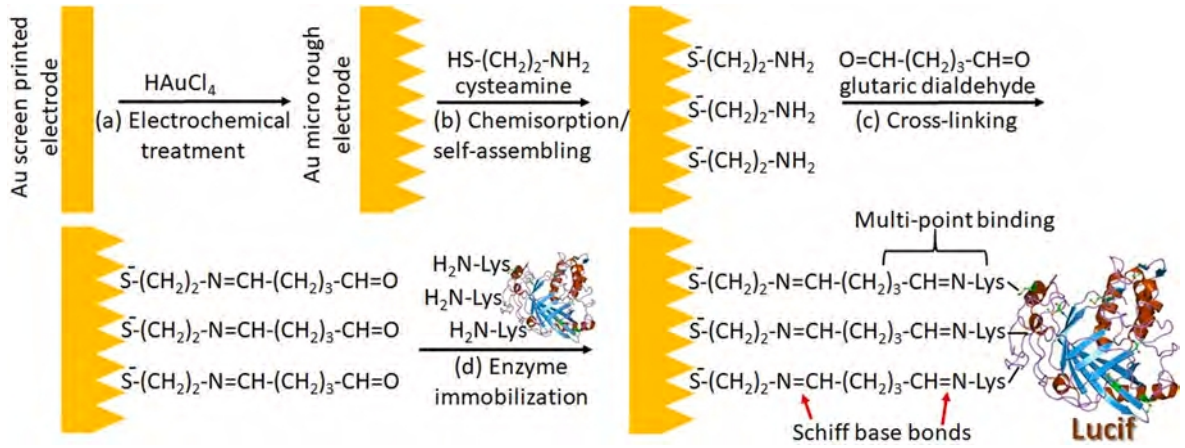


**Scheme 2.** Stepwise immobilization of luciferase enzyme at the electrode surface. Another way of the luciferase immobilization used in control experiments is outlined in Figure SD2 in the Supplementary Data.

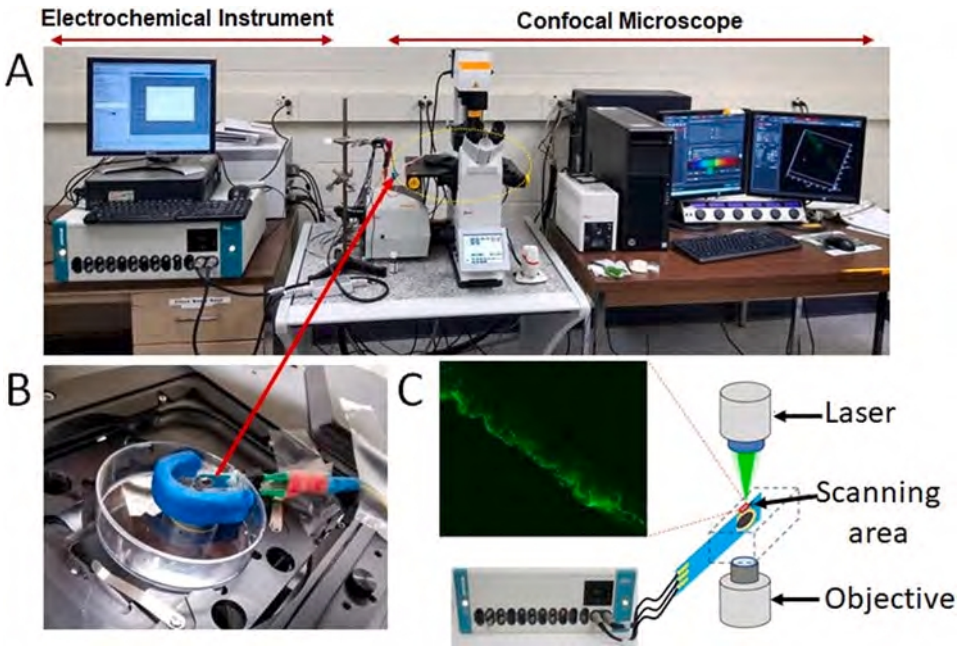


**Fig. 2.** (A) The experimental setup used for the confocal microscope study of the bioluminescence controlled by the electrochemical reduction of $O_2$. (B) Close view of the electrochemical cell located in the optical chamber of the confocal microscope. (C) Schematics of the electrochemical cell and optical system. Note that the electrode surface was arranged in parallel to the optical path, thus allowing fluorescent analysis of processes at the electrode surface.

quasi-reference electrodes. The Au working electrode is composed of inhomogeneous mixture of Au micro-particles (see a scanning electron microscopy (SEM) image of the Au surface at the company website: http://www.dropsens.com/en/pdfs_productos/new_brochures/gold_electrodes.pdf). The DRP 220BT SPGEs are specifically designed to work in a solution by entirely immersing the sensing area. Prior to their modification, the SPGEs were pre-treated by cyclic voltammetry (30 cycles at 100 mV/s) in the potential range of 0 and +1.6 V (vs. Ag|AgCl|KCl, 3 M, reference electrode) in 0.5 M $H_2SO_4$. Afterwards, SPGEs were modified by electrodeposition of highly porous gold (hPG) by initially sweeping the potential for 30 scans between +0.8 and 0 V at a scan rate of 50 mV $s^{-1}$ and then applying a fixed potential of −3 V in a 10 mM $HAuCl_4$ - solution containing 2.5 M $NH_4Cl$ for 150 sec [29,30]. The color of the working electrode turned to black. Then, the electrode was immersed in water and shaken at low speed for one minute. The real surface area of the porous Au electrode was determined from the cathodic peak (at ca. 0.8 V) corresponding to the reduction of the gold oxide layer upon performing cyclic voltammetry in 0.5 M $H_2SO_4$ solution and compared it with the original (as supplied) gold electrode. Cyclic voltammetry performed in 10 mM TRIS buffer, pH 7.8, with added 100 mM $Na_2SO_4$ in the potential range of 0 and −1.0 V at scan rate of 2 mV/s was used to analyze $O_2$ electrochemical reduction under air and Ar.

### 2.4. Immobilization of luciferase on the highly porous SPGEs

The highly porous gold (hPG) electrodes were first modified by chemisorption of a self-assembled cysteamine monolayer [31], then introducing amino groups available for the next modification steps. The hPG electrodes were reacted with 50 μL of cysteamine solution (100 mM) for 1 h and then rinsed with water to remove the unbound cysteamine. Then, the cysteamine monolayer-modified electrodes were reacted with a glutaric dialdehyde solution, which was prepared by mixing 50 μL (2.5% v/v) aqueous glutaric dialdehyde with 950 μL 20 mM HEPES buffer, pH 6.2, containing 30% v/v ethanol. After reacting

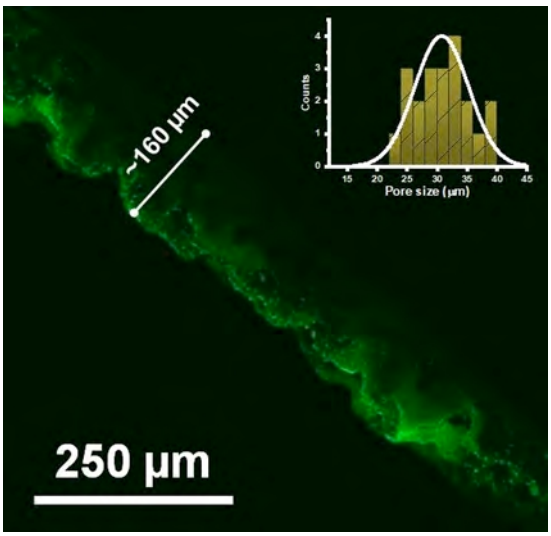


**Fig. 3.** A confocal microscope image of the luciferase-modified electrode with no potential applied and no substrates added (the background fluorescence). The inset shows the pore-size distribution derived from the image.

the electrodes with the solution of glutaric dialdehyde for 2 hrs, the modified electrodes were rinsed with the HEPES buffer (20 mM, pH 6.2). The procedure resulted in the formation of aldehyde groups at the electrode surface available for the enzyme immobilization. Finally, the electrodes were reacted with a luciferase buffer solution (10 µL, 2 mg/mL) for 2 hrs, resulting in the enzyme covalent immobilization as a monolayer. The enzyme-modified electrodes were rinsed with TRIS buffer (10 mM, pH 7.8) and kept overnight at 4 °C under dark prior to their use. Another way of luciferase immobilization used in control experiments is outlined in Figure SD2 in the Supplementary Data.

### 2.5. Confocal microscope measurements

The confocal microscope measurements were performed differently for the analysis of the local pH near the electrode surface and for measurements of the bioluminescence activity of the immobilized luciferase. The pH analysis near the electrode surface was performed by measuring fluorescence of the pH sensitive dye (FAM345) as detailed in our recent comprehensive study [28]. A solution of FAM345 (10 µM) in TRIS buffer (10 mM, pH 7.8) in the presence of 100 mM of $Na_2SO_4$ and $O_2$ under equilibrium with air was used for the local (interfacial) pH analysis. The dye fluorescence was measured in the range of 500–700 nm with the excitation wavelength 405 nm. Quantitative analysis of the confocal microscope images was performed by analyzing the green color intensity and distribution using ImageJ software. The luciferase bioluminescence was measured in the solution composed of D-luciferin (10 µM), ATP (0.25 µM), and $MgCl_2$ (5 µM) in TRIS buffer (10 mM, pH 7.8) in the presence of 100 mM of $Na_2SO_4$ and $O_2$ under equilibrium with air (3 mL total volume). The confocal fluorescent images of the modified

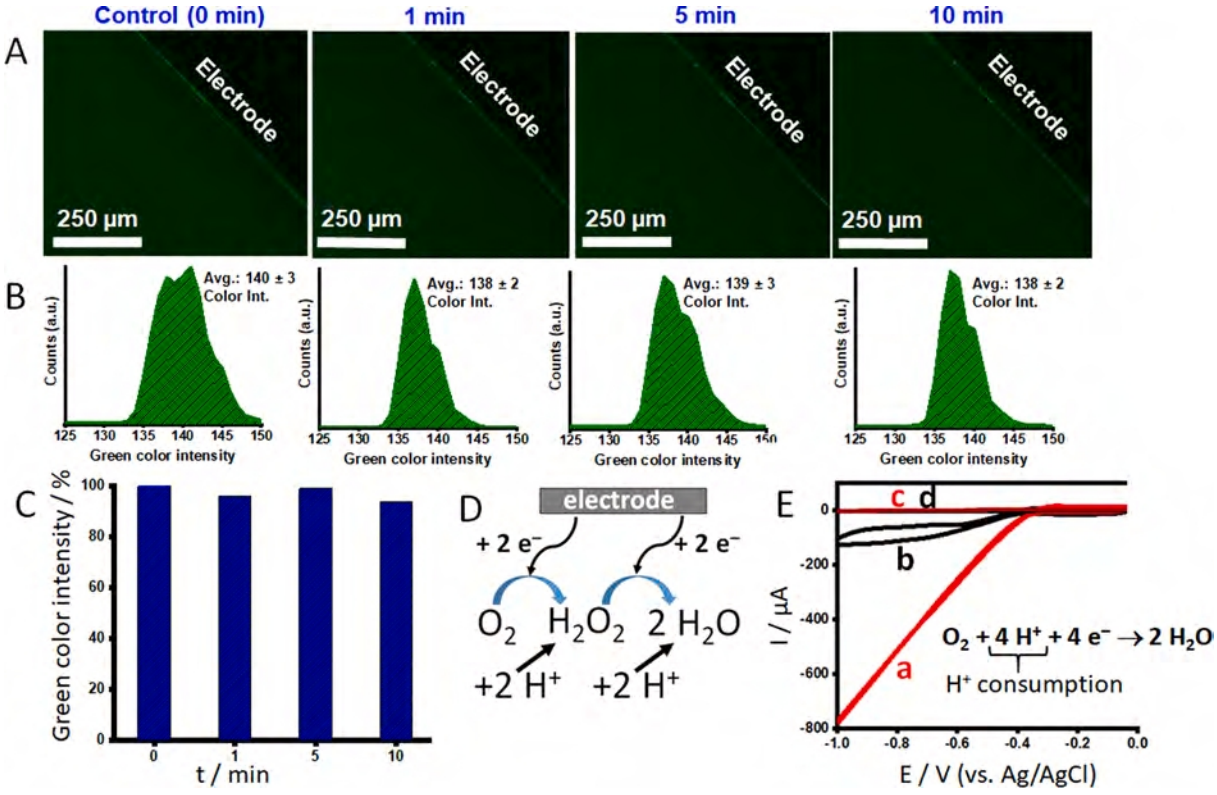


**Fig. 4.** (A) Confocal microscope images obtained after different time-intervals of applying potential −0.9 V (vs. a quasi-reference electrode in the SPGE assembly). The solution included FAM345 (10 µM) in TRIS buffer (10 mM, pH 7.8) in the presence of 100 mM of $Na_2SO_4$ and $O_2$ under equilibrium with air. (B) Analysis of the green color in the images shown in (A). (C) A bar-chart showing green color intensity after different time of applying potential −0.9 V (vs. a quasi-reference electrode). The bars were calculated from the color distribution plots shown in (B). (D) Schematics of the electrochemical reduction of $O_2$ resulting in production of $H_2O_2$ or $H_2O$ depending on the potential applied. The 4-electron reduction resulting in the $H_2O$ formation is a dominating process at the potential of −0.9 V. (E) Cyclic voltammograms corresponding to the electrochemical reduction of $O_2$: (a) in the presence of $O_2$ under equilibrium with air recorded with the hPG electrode; (b) measured under Ar with the hPG electrode (note incomplete $O_2$ removal because of the electrode porosity); (c-d) cyclic voltammograms recorded under air and Ar with the original SPGE (note indistinguishable current in the used current scale). The solution was composed of TRIS buffer (10 mM, pH 7.8) with 100 mM $Na_2SO_4$. Potential scan rate was 2 mV/s. The potentials are shown vs. Ag|AgCl|KCl, 3 M, reference electrode. (For interpretation of the references to color in this figure legend, the reader is referred to the web version of this article.)

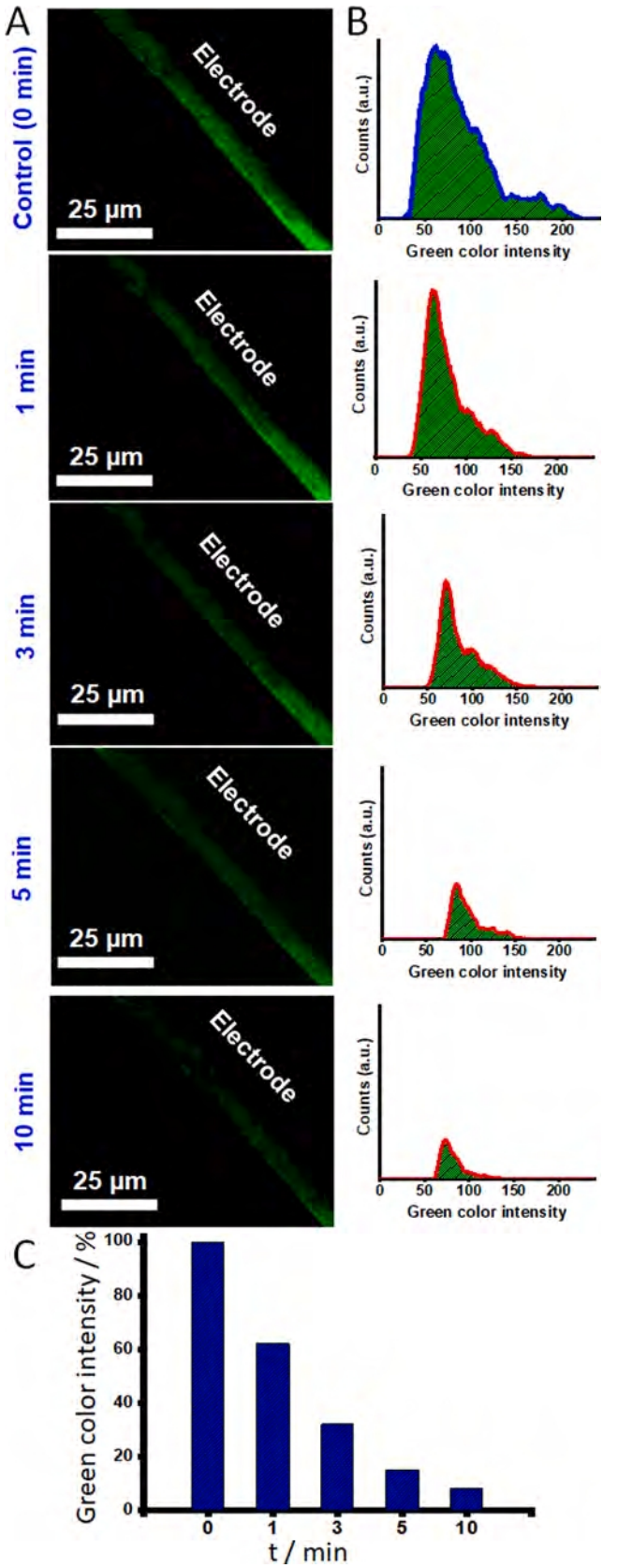


*(caption on next column)*

**Fig. 5.** Confocal microscope images (A) and the corresponding green color intensity (B) obtained with the luciferase-modified electrode after different time of the −0.9 V potential applied (vs. a quasi-reference electrode). The solution included D-luciferin (10 μM), ATP (0.25 μM), and $MgCl_2$ (5 μM) in TRIS buffer (10 mM, pH 7.8) in the presence of 100 mM of $Na_2SO_4$ and $O_2$ under equilibrium with air. (C) The bar-chart showing decrease of the bioluminescence intensity with the increasing time of the potential applied. The bars are derived from the plots shown in (B). Local (interfacial) $O_2$ concentration decrease upon the potential application is shown in Figure SD1 in the Supplementary Data. (For interpretation of the references to color in this figure legend, the reader is referred to the web version of this article.)

luciferase/hPG electrode were recorded in the range of 500–700 nm and analyzed with the ImageJ software. The bioluminescence measurements were performed with the applied potential −0.9 V (vs. a quasi-reference electrode of the SPGE assembly) and upon releasing the applied potential.

## 3. Results and discussion

Oxidative decarboxylation of D-luciferin catalyzed by luciferase enzymes results in formation of a singlet excited state of oxyluciferin, which then produces light emission ($\lambda_{max}$ = 560 nm) as it relaxes to the ground state [26], Scheme 1A. The biocatalytic reaction resulting in the luminescence requires presence of the enzyme co-substrates, ATP and molecular oxygen ($O_2$), as well as $Mg^{2+}$ cations as promoters. Obviously, the rate of the biocatalytic transformation and then the luminescence intensity both depend on concentrations of the reacting species. It is very difficult to change concentrations of D-luciferin or $Mg^{2+}$ cations by any external signals, particularly electrochemically, however, it is very easy to decrease $O_2$ concentration by its electrochemical reduction. While bulk reduction of dissolved $O_2$ is a time-consuming process, its local depletion near an electrode surface is much faster. Therefore, the bioluminescence process controlled electrochemically was studied using an electrode-immobilized luciferase enzyme (Scheme 1B). The enzyme immobilization is also highly important for any of its bioelectronic application.

The Au electrode support for the enzyme immobilization was pretreated electrochemically (see the Experimental section 2.3), resulting in a highly porous interface with dramatically increased electrochemically active surface (Fig. 1B) compared with the original screen printed Au electrode (SPGE) (Fig. 1A). The size of the produced pores was in the range of 15–40 μm (Fig. 1C). The corresponding 3D-surface mapping of the electrode surface confirmed the porosity (Fig. 1D), providing consistency with the obtained SEM image. The surface increase by factor ca. 50 was determined electrochemically by performing cyclic voltammetry with oxidative deposition of a gold oxide monolayer on the electrode surface, then followed by its reductive striping [32]. The real electrode surface (taking into account its roughness) is measurable as a charge (integrated current) under the cathodic peak in the cyclic voltammograms (Fig. 1E and 1F for the initial and roughed electrodes, respectively). The electrode surface roughening allowed significant increase of the amount of the surface-bound luciferase enzyme.

The luciferase immobilization proceeded in several steps, starting from self-assembling of a cysteamine monolayer, then continued with reacting amino groups with glutaric dealdehyde as a homobifunctional cross-linker (Scheme 2). Finally, the amino groups of the lysine residues of luciferase reacted with aldehyde groups of the surface-bound glutaric dialdehyde. Notably, the Schiff-base bonds produced at the surface upon reacting aliphatic amines and aldehydes are not stable (their formation is reversible) [33], however, the enzyme immobilization is stable due to the multiple-point binding [17]. The luciferase-modified electrodes were studied with a setup which included an electrochemical instrument for applying potential on the electrode and a confocal microscope for *operando* measurements of the luminescence generated at the electrode surface (Fig. 2). The background fluorescence emitted from the

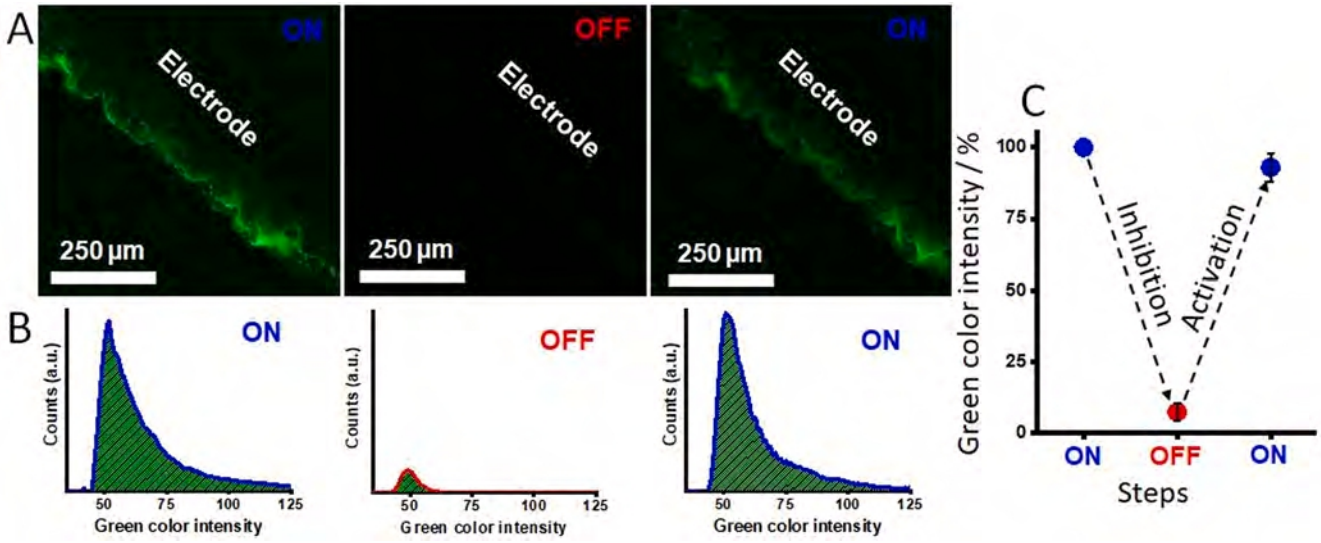


**Fig. 6.** (A) Confocal microscope images showing the bioluminescence produced by the immobilized luciferase with no potential applied (ON state) for 5 min and after −0.9 V potential applied for 10 min (OFF state). (B) Green color intensity corresponding to the bioluminescence in the ON and OFF states. (C) The reversible inhibition and re-activation of the bioluminescence upon applying and removing −0.9 V potential applied. The solution included D-luciferin (10 μM), ATP (0.25 μM), and $MgCl_2$ (5 μM) in TRIS buffer (10 mM, pH 7.8) in the presence of 100 mM of $Na_2SO_4$ and $O_2$ under equilibrium with air. (For interpretation of the references to color in this figure legend, the reader is referred to the web version of this article.)

luciferase-modified electrode surface reflected the electrode roughness, further confirming measurements with the SEM imaging and 3D-surface mapping analysis (Fig. 3).

Remembering the goals of the project, one should note that the rate of the biocatalytic process and therefore the luminescence intensity both depend on the $O_2$ local concentration near the electrode surface (Scheme 1B). However, there is another experimental parameter which can affect the reaction rate – it is the local pH value. Indeed, the electrochemical $O_2$ reduction is accompanied with consumption of $H^+$ ions potentially resulting in significant local pH increase [28]. It is known [34] that the biocatalytic activity of luciferase is pH dependent, increasing with the pH elevation. Therefore, the increase of the enzyme activity with the increasing local pH may compensate, at least partially, the $O_2$ local concentration depletion upon its electrochemical reduction. Thus, special attention should be paid to avoiding the pH variation in the course of the experiments. The local pH changes produced by electrochemical reactions are allowed only when a weak buffer is present in the solution. Increasing the buffer concentration suppresses the pH changes, as expected [28]. Therefore, the experiments were performed in the presence of TRIS buffer (10 mM, pH 7.8), assuming [28] that this buffer concentration should be high enough to preserve the local pH when $O_2$ reduction proceeds (Fig. 4D). Indeed, Fig. 4A-C shows the same (unchanged) fluorescence of the pH-sensitive dye (FAM345) during the electrochemical reduction of $O_2$ upon applying potential −0.9 V on the working electrode. This control experiment confirmed that the used buffer concentration is high enough to keep the interfacial (near the electrode surface) pH unchanged. In case the local pH had changed, the dye fluorescence would have changed, as reported in our recent comprehensive study [28]. This result is important to confirm that only one experimental parameter (i.e. $O_2$ concentration) is changing under the used experimental conditions, while the local pH is not affected due to the high buffer concentration. It should be noted that the effect of the electric field on the enzyme activity can be excluded due to the high ionic strength of the background electrolyte solution (control experiments are outlined in Figure SD3 in the Supplementary Data).

Cyclic voltammograms demonstrated $O_2$ reduction at the potentials more negative than −0.3 V (vs. Ag|AgCl|KCl, 3 M) (Fig. 4E). Notably, the $O_2$ reduction was the only electrochemical process in the used potential range. Then, the constant potential electrochemical $O_2$ reduction was performed at −0.9 V, when the current is large enough for the effective depletion of $O_2$ near the electrode surface. It is well known [35] that electrochemical $O_2$ reduction proceeds in several steps, where the major intermediate product is $H_2O_2$. The final product is $H_2O$ produced upon reduction of $H_2O_2$ (Fig. 4D). The confocal imaging of the interface in the presence of the pH-sensitive fluorescent dye confirmed the unchanged pH value in the presence of the used buffer, as explained above (Fig. 4A-C). Then, after confirming that the pH effect is excluded, the experiments were directed to the reversible control of the luciferase activity with the electrochemical signals applied.

Fig. 5 shows decreasing luminescence with the increasing time of the potential (−0.9 V) applied. The result can be interpreted as the effect of decreasing local $O_2$ concentration due to its reductive consumption. The experimental observation of the $O_2$ depletion at the electrode surface was performed using chronoamperometric measurements of the $O_2$ reduction; see Figure SD1 in the Supplementary Data. It should be noted that the constant potential electrolysis (performed in the chronoamperometric regime) demonstrated the measured current decay almost to the background current value, thus demonstrating the complete depletion of $O_2$ near the electrode surface. Importantly, the experiment demonstrates tunable bioluminescence intensity controlled by the electrochemical signal applied over time. Even more impressive result was obtained when the potential was applied and released in a cyclic mode resulting in the reversible inhibition and then re-activation of the bioluminescence, respectively (Fig. 6). The cyclic ON-OFF changes of the luciferase luminescence was repeatable as long as $O_2$ local concentration could be variated.

The enzyme-functionalized electrodes were stable for at least 10 days (data not shown) stored in the refrigerator (4–8 °C) and under dark conditions.

## 4. Conclusions and perspectives

The obtained results demonstrated reversible tuning and switching of the immobilized luciferase activity observed as the variable signal-controlled luminescence. The applied signal was an electric potential resulting in reversible depletion of $O_2$ in a thin film near the electrode surface. The studied system is an additional example to the large collection of previously reported signal-controlled electrochemical systems [13]. However, the use of the light emitting biochemical system has important difference from the previously studied enzymes. While

most of enzymes produce reactants in course of time and the products need to be accumulated in the bulk solution for their assay, the bioluminescence can be detected immediately, directly from the modified interface, thus allowing the *operando* experiments. The tunable luciferase activity was studied by applying the reductive potential for different time-intervals (Fig. 5). In addition, the precise tuning of the luciferase activity can be achieved by changing the applied potential or current under potentiostatic or galvanostatic regimes, respectively. The relatively high reductive potential (−0.9 V) applied in the study can be significantly decreased when $O_2$ reduction is biocatalyzed by bilirubin oxidase or laccase [36,37]. The bioelectrochemical reduction of $O_2$ can proceed at very mild potentials near 0 V (vs. Ag/AgCl). This approach requires co-immobilization of the $O_2$-reducing enzymes and luciferase. While recently we reported on enzyme activity reversibly controlled by local (interfacial) pH changes produced electrochemically [10], the present study demonstrated another than pH variation mechanism of switching and tuning enzyme activity. Overall, the present preliminary study has possible extensions to many other realizations of the switchable and tunable bioluminescent systems and potential practical applications.

## Declaration of Competing Interest

The authors declare that they have no known competing financial interests or personal relationships that could have appeared to influence the work reported in this paper.

## Acknowledgement

This work was supported by the NSF award 1939063 to EK. This paper is dedicated to the memory of Prof. Artem Melman (deceased in 2021) who was one of the leading scientists working with our team. AO acknowledges the Colin Garfield Fink Postdoctoral Summer Fellowship awarded by the Electrochemical Society.

## Appendix A. Supplementary data

Supplementary data to this article can be found online at https://doi.org/10.1016/j.bioelechem.2022.108109.

## References

[1] S. Choi (Ed.), Systems Biology for Signaling Networks, Springer-Verlag, New York, 2010.
[2] J. Hancock, Cell Signalling, third ed.,, Oxford University Press, 2010.
[3] S. Szunerits, F. Teodorescu, R. Boukherroub, Electrochemically triggered release of drugs, Eur. Polym. J. 83 (2016) 467–477.
[4] E. Katz, M. Pita, Biofuel cells controlled by logically processed biochemical signals: towards physiologically regulated bioelectronic devices, Chem. Eur. J. 15 (2009) 12554–12564.
[5] E. Katz, Enzyme-Based Computing Systems, Wiley-VCH, Weinheim, 2019.
[6] E. Katz (Ed.), Biomolecular Information Processing - From Logic Systems to Smart Sensors and Actuators, Wiley-VCH, Weinheim, 2012.
[7] E. Katz, J.M. Pingarrón, S. Mailloux, N. Guz, M. Gamella, G. Melman, A. Melman, Substance release triggered by biomolecular signals in bioelectronic systems, J. Phys. Chem. Lett. 6 (2015) 1340–1347.
[8] W. Zhang, T. Ji, Y. Li, Y. Zheng, M. Mehta, C. Zhao, A. Liu, D.S. Kohane, Light-triggered release of conventional local anesthetics from a macromolecular prodrug for on-demand local anesthesia, Nature Commun. 11 (2020) 2323.
[9] S. Carregal-Romero, P. Guardia, X. Yu, R. Hartmann, T. Pellegrino, W.J. Parak, Magnetically triggered release of molecular cargo from iron oxide nanoparticle loaded microcapsules, Nanoscale 7 (2015) 570–576.
[10] V.K. Kadambar, M. Bellare, P. Bollella, E. Katz, A. Melman, Electrochemical control of catalytic activity of immobilized enzymes, Chem. Commun. 56 (2020) 13800–13803.
[11] S. Goggins, B.J. Marsh, A.T. Lubben, C.G. Frost, Signal transduction and amplification through enzyme-triggered ligand release and accelerated catalysis, Chem. Sci. 6 (2015) 4978–4985.
[12] M. Gamella, Z. Guo, K. Alexandrov, E. Katz, Bioelectrocatalytic electrodes modified with PQQ-glucose dehydrogenase–calmodulin chimera switchable by peptide signals: pathway to generic bioelectronic systems controlled by biomolecular inputs, ChemElectroChem 6 (2019) 638–645.
[13] E. Katz, Signal-Switchable Electrochemical Systems - Materials, Methods, and Applications, Wiley-VCH, Weinheim, 2018.
[14] I. Willner, E. Katz (Eds.), Bioelectronics: From Theory to Applications, I. Willner, Wiley-VCH, Weinheim, 2005.
[15] E. Katz (Ed.), Implantable Bioelectronics - Devices, Materials and Applications, Wiley-VCH, Weinheim, 2014.
[16] J. Kim, I. Jeerapan, J.R. Sempionatto, A. Barfidokht, R.K. Mishra, A.S. Campbell, L. J. Hubble, J. Wang, Wearable bioelectronics: enzyme-based body-worn electronic devices, Acc. Chem. Res. 51 (2018) 2820–2828.
[17] I. Willner, E. Katz, Integration of layered redox-proteins and conductive supports for bioelectronic applications, Angew. Chem. Int. Ed. 39 (2000) 1180–1218.
[18] N.G. Welch, Orientation and characterization of immobilized antibodies for improved immunoassays, Biointerphases 12 (2017) 02D301.
[19] S. Seetharaman, M. Zivarts, N. Sudarsan, R.R. Breaker, Immobilized RNA switches for the analysis of complex chemical and biological mixtures, Nature Biotechnol. 19 (2001) 336–341.
[20] P. Bollella, E. Katz, Biosensors – recent advances and future challenges, Sensors 20 (2020) 6645.
[21] V. Naresh, N. Lee, A review on biosensors and recent development of nanostructured materials-enabled biosensors, Sensors 21 (2021) 1109.
[22] T. Azad, H.J.J. van Rensburg, J. Morgan, R. Rezaei, M.J.F. Crupi, R. Chen, M. Ghahremani, M. Jamalkhah, N. Forbes, C. Ilkow, J.C. Bell, Luciferase-based biosensors in the era of the COVID-19 pandemic, ACS Nanosci. Au 1 (2021) 15–37.
[23] S.K. Elledge, X.X. Zhou, J.R. Byrnes, A.J. Martinko, I. Lui, K. Pance, S.A. Lim, J. E. Glasgow, A.A. Glasgow, K. Turcios, N.S. Iyer, L. Torres, M.J. Peluso, T. J. Henrich, T.T. Wang, C.M. Tato, K.K. Leung, B. Greenhouse, J.A. Wells, Engineering luminescent biosensors for point-of-care SARS-CoV-2 antibody detection, Nature Biotechnol. 39 (2021) 928–935.
[24] Y. Zhang, X. Ke, C. Zheng, Y. Liu, L. Xie, Z. Zheng, H. Wang, Development of a luciferase-based biosensor to assess enterovirus 71 3C protease activity in living cells, Sci. Rep. 7 (2017) 10385.
[25] S.J. Gould, S. Subramani, Firefly luciferase as a tool in molecular and cell biology, Anal. Biochem. 175 (1988) 5–13.
[26] A.J. Syed, J.C. Anderson, Applications of bioluminescence in biotechnology and beyond, Chem. Soc. Rev. 50 (2021) 5668–5705.
[27] V.F. Valuk, G. Duportail, V.G. Pivovarenko, A wide-range fluorescent pH-indicator based on 3-hydroxyflavone structure, J. Photochem. Photobiol. A 175 (2005) 226–231.
[28] P. Bollella, A. Melman, E. Katz, *Operando* local pH mapping of electrochemical and bioelectrochemical reactions occurring at an electrode surface: Effect of the buffer concentration, ChemElectroChem 8 (2021) 3923.
[29] P. Bollella, Y. Hibino, K. Kano, L. Gorton, R. Antiochia, Highly sensitive membraneless fructose biosensor based on fructose dehydrogenase immobilized onto aryl thiol modified highly porous gold electrode: Characterization and application in food samples, Anal. Chem. 90 (2018) 12131–12136.
[30] P. Bollella, Porous gold: a new frontier for enzyme-based electrodes, Nanomaterials 10 (2020) 722.
[31] E. Katz, A.A. Solov'ev, Chemical modification of platinum and gold electrodes by naphthoquinones using amines containing sulfhydryl or disulphide groups, J. Electroanal. Chem. 291 (1990) 171–186.
[32] B.E. Conway, Electrochemical oxide film formation at noble metals as a surface-chemical process, Prog. Surf. Sci. 49 (1995) 331–452.
[33] M.S. Hossain, P.K. Roy, R. Ali, C.M. Zakaria, M. Kudrat-E-Zahan, Selected pharmacological applications of 1st row transition metal complexes: a review, Clinical Med. Res. 6 (2017) 177–191.
[34] J.F. Thompson, K.F. Geoghegan, D.B. Lloyd, A.J. Lanzetti, R.A. Magyar, S. M. Anderson, B.R. Branchini, Mutation of a protease-sensitive region in firefly luciferase alters light emission properties, J. Biol. Chem. 272 (1997) 18766–18771.
[35] K.J. Vetter, Electrochemical Kinetics – Theoretical Aspects, first ed., Elsevier, New York, 1967.
[36] M. Bellare, V. Krishna Kadambar, P. Bollella, E. Katz, A. Melman, Molecular release associated with interfacial pH change stimulated by a small electrical potential applied, ChemElectroChem 7 (2020) 59–63.
[37] C. Vaz-Dominguez, S. Campuzano, O. Rüdiger, M. Pita, M. Gorbacheva, S. Shleev, V.M. Fernandez, A.L. De Lacey, Laccase electrode for direct electrocatalytic reduction of $O_2$ to $H_2O$ with high-operational stability and resistance to chloride inhibition, Biosens. Bioelectron. 24 (2008) 531–537.